A Thesis Submitted to the Sylhet Engineering College for the Degree of
Bachelor of Science in Electrical and Electronic Engineering

Development and Performance Analysis of Non-Toxic Tin-Based Perovskite Solar Cells

By
Safwan Bin Waris
Arnab Datta
&
Faiyan Chowdhury

Supervised by,
Dr. Md. Shahid Iqbal
Associate Professor and Head
Department of Electrical and Electronic Engineering
Sylhet Engineering College

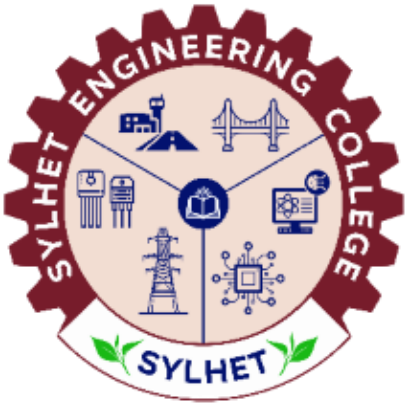

June, 2025
Sylhet Engineering College, Sylhet
Affiliated with
Shahjalal University of Science & Technology (SUST)

The thesis titled "**Development and Performance Analysis of Non-Toxic Tin-Based Perovskite Solar Cells**" submitted by Safwan Bin Waris, Arnab Datta, Faiyan Chowdhury; Student ID: 2019338505, 2019338512 and 2018338553; Session 2019-2020, to the Department of Electrical and Electronic Engineering, Sylhet Engineering College, has been accepted as satisfactory in partial fulfillment of the requirement for the Degree of Bachelor of Science in Electrical and Electronic Engineering and approved as to its style and contents.

BOARD OF EXAMINERS

_____
Md. Shahid Iqbal
Assistant Professor and Head
Department of Electrical and Electronic Engineering
Sylhet Engineering College, Sylhet.

Chairman
& Supervisor

_____
Salman Fazle Rabby
Assistant Professor
Department of Electrical and Electronic Engineering
Sylhet Engineering College, Sylhet.

Member

_____
Apurba Biswas
Assistant Professor
Department of Electrical and Electronic Engineering
Sylhet Engineering College, Sylhet.

Member

_____
Md. Ashraful Alam
Lecturer
Department of Electrical and Electronic Engineering
Sylhet Engineering College, Sylhet.

Member

_____
Mahedi Kamal Ahmed
Lecturer
Department of Electrical and Electronic Engineering
Sylhet Engineering College, Sylhet.

Member

_____
Arif Ahammad
Assistant Professor
Department of Electrical and Electronic Engineering
Shahjalal University of Science & Technology, Sylhet

Member
(External)

Acknowledgement

First and foremost, we appreciate the Most Gracious and Merciful Almighty. He showered us with blessings, providing us with courage and support during the most challenging parts of completing this dissertation.

We would like to express our sincere appreciation to our esteemed supervisor, **Md. Shahid Iqbal**, Assistant Professor and Head of the Department of Electrical and Electronic Engineering at Sylhet Engineering College. His invaluable academic mentorship, exemplary leadership, positive encouragement, insightful advice, and unwavering support have been instrumental throughout our academic pursuit. We are truly grateful for his guidance. Furthermore, we extend our thanks to our other faculty members**, Salman Fazle Rabby** and **Md. Ashraful Alam** for their kindness, support, and cooperation during our academic journey. Their assistance has been greatly appreciated.

Lastly, we thank our parents, dearest siblings and friends for their unconditional love and continuous support. Without the mental strength you provided, surviving the journey full of ups and downs would not have been possible.

Abstract

Lead-free perovskite methylammonium tin halide ($CH_3NH_3SnI_3$) solar cell has been numerically simulated in SCAPS-1D software. The research subjects were different compositions, absorber thickness, and absorber bandgap. The optimal performance for $CH_3NH_3PbI_3$ with NiO_x Hole Transport Material (HTM), and ZnO Electron Transport Material (ETM) indicated an overall efficiency of 18.22%, FF of 81.79%, J_{sc} of 20.94mA/cm2, and V_{oc} of 1,06V. For the Tin, lead-free halide CH3NH3SnI3 the best outcome shows an overall efficiency of 25.73%, an FF of 81.06%, a J_{sc} of 32.55mA/cm2, and a V_{oc} of 0.97V. Due to lead toxicity, lead-free PSC offers an advantage over lead-based PSC. The absorber layer's graded bandgap structure was also used to boost the PSC's effectiveness further.

Keywords: Perovskite Solar cell, lead-free, bandgap, SCAPS-1D, Hole Transport Material (HTM), Electron Transport Material (ETM).

Table of Content

List of Figures

List of Tables

Nomenclature

ATM 1.5 SUN	Air mass of 1.5 atmosphere & Solar zenith angle of 48.2°
ETL	Electron transporting layer
EQE	External quantum efficiency
EXITON	Exited electron-hole pair
FF	Fill Factor
FIB	Focused ion beam
HTL	Hole transporting layer
ISC	Short circuit current density V=0
IV CURVE	Current-voltage curve
Jsc	Short circuit current density V=0
M	Molarity is also known as molar concentration, mole/volume.
PSC	Perovskite Solar cell
PCE	Power conversion Efficiency
Voc	Open circuit voltage,I=0

Chapter 01: Introduction

1.1 Overview

This thesis provides a comprehensive overview of the fundamental principles underlying solar cell operation, focusing on charge generation, electron-hole transport, and light absorption. It examines the structure and function of typical solar cells, highlighting the roles of the absorber layer, hole transport material (HTM), and electron transport material (ETM). The study emphasizes perovskite materials, comparing lead-based and lead-free variants, and explores their performance, stability, and environmental impact. Key characterization methods, including current-voltage measurements and equivalent circuit modeling, are discussed to assess device efficiency. Critical factors such as recombination effects, quantum efficiency, and the selection of optimal HTM and ETM materials are analyzed. Additionally, the influence of absorber bandgap, thickness, and operational conditions on perovskite solar cell performance is investigated, providing guidance for designing efficient, stable, and sustainable photovoltaic modules.

1.2 Objective

The main objective of the research is on lead-free perovskite solar cells. This thesis performs extensive device simulations to optimize PSC conversion efficiencies, minimize losses, and reach higher efficiency. In addition, the aim of the work is briefly stated as follows:

Objective- 1 Replacing the lead-based PSC with a suitable lead-free absorber layer.

Objective- 2 To increase the efficiency of perovskite solar cells by finding the appropriate Voc, bandgap, thickness, and temperature.

Objective- 3 Finding the best HTM and ETM for a lead-free perovskite layer.

Objective- 4 Increasing stability by changing ETM, HTM and inner parameters of ETM and HTM.

1.3 Physics of Solar Cell

Materials used in semiconductors, which can absorb photons and produce energy, make up solar cells. To create a photocurrent and power an external load, the absorbed photons in the semiconductor split into free charge carriers that move in a specific direction. Simply put, a solar cell is a semiconducting material precisely constructed to absorb solar light effectively and transform it into electrical energy. A schematic of a basic solar cell is displayed in Figure 1.1

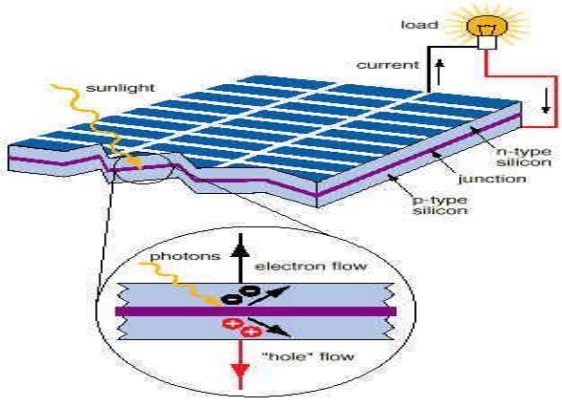

Fig1.1 Basic solar cell.

The cell's materials include a metallic grid front electrode, an anti-reflective coating sometimes, two types of semiconducting material—n-type and p-type—for the active layers, and a metallic electrode functioning as the bottom contact. Positively doped materials are called p-type materials, and materials with more electrons are called n-type materials. Light enters the front of the solar cell from above. One of the diode's electrical contacts is a metallic grid, which lets light pass through the grid lines onto the semiconductor, which is absorbed and transformed into electrical energy. It is possible to imagine the existence of all electromagnetic radiation, including sunlight, as being made up of particles referred to as photons, the power of which is based on the spectral properties of its source. The photon energy, E, can be written in terms of frequency of light as:

$$E_v = h\nu$$

Photons also display a wavelike character, and the energy of photons Eλ can be expressed in terms of wavelength, λ by:

$$E\lambda = hc/\lambda$$

Where c is the velocity of light, v is the frequency of the photon, h is Plank's constant, and λ is the photon's wavelength. The negatively charged particle will go in the preferred direction of the p-type material to produce an electron-hole pair when photons with enough power enter and knock one of the electrons loose. The gradient between the n-type and p-type materials generates an electric field. This field of electricity causes charges to flow in one direction, which results in current flow. The energy conversion process will only be assisted by photons that contain sufficient power to form an electron-hole pair or photons with an energy level that exceeds the bandgap of semiconductors. Thus, when developing efficient solar cells, the spectrum of sunlight must be considered. In general, the electrons in the conduction band of an n-type semiconductor get pushed toward the electrode with the positive terminal when the difference in potential is applied across it. The n-type conductivity of the semiconducting material is defined as the current flow through negative free charge carriers, which is caused by the electrons leaving holes in the valence band. Corresponding to this, with the p-type material, the electrode with the negative terminal is the target of holes created in the valence band. P-type conductivity is the current flow through a positively charged carrier known as a hole in a p-type material.

Chapter 02: Relevant Work

A comparison of some literature studied to determine the working approach is provided below.
Salih et al. (2023) developed a highly efficient tin halide–based perovskite solar cell with a planar structure. Their work demonstrated the potential of lead-free absorbers such as $CH_3NH_3GeI_3$, $CH_3NH_3PbI_3$, and $CH_3NH_3SnI_3$, achieving a fill factor of 71.30% and an impressive efficiency of 24.54% using TiO as the hole transport material (HTM) and CuO_2 as the electron transport material (ETM) [4].

Mandadapu et al. (2017) emphasized the effect of absorber thickness and defect concentration on device performance. Their study revealed that doping concentration in both HTM and ETM could significantly enhance photovoltaic parameters, resulting in a fill factor of 81.58% and an efficiency of 31.77%. The device structure used PEDOT:PSS as the HTM, SnO_2 as the ETM, and $CH_3NH_3PbI_3$ as the absorber [8].

Rahman et al. (2019) focused on transport material properties as key determinants of PSC performance. Their analysis showed that ZnO was the most suitable ETM compared to Cu_2O and SnO_2, when combined with NiOx as HTM and $MAPbI_3$ as absorber. This configuration achieved a fill factor of 76.78% and an efficiency of 17.84% [5]. A related study by **Ghosh et al. (2019)** investigated the influence of absorber thickness using $CH_3NH_3PbI_3Br$ as the active layer, where the device delivered a fill factor of 75.96% and an efficiency of 18.22% with NiOx as HTM and ZnO as ETM [6].

Kumavat et al. (2017) provided comprehensive insights into the factors influencing the fill factor and efficiency of PSCs. Their review served as a guide for organic chemistry researchers in identifying suitable molecules for device improvement. The representative device discussed used TiO_2 as HTM, SnO_2 as ETM, and $CH_3NH_3PbI_3$ as absorber, achieving a fill factor of 75.58% and efficiency of 21.77% [7].

Srivastava et al. (2022) explored lead-free alternatives, suggesting $MASnI_3$ as a promising non-toxic replacement for lead-based materials. Their work highlighted its capability as a high-contrast alternative to $MAPbX_3$, achieving a fill factor of 77.79% and efficiency of 17.45% when paired

with NiOx as HTM and TiO_2 as ETM [3]. Similarly, **Singh et al. (2020)** provided in-depth insights into improvement strategies for tin- and germanium-based lead-free perovskites, reporting a fill factor of 62.71% and an efficiency of 24.54% using $CH_3NH_3SnI_3$ as absorber with TiO as HTM and SnO_2 as ETM [1].

Wu et al. (2021) highlighted the excellent optoelectronic properties of organic–inorganic lead halide perovskites, including high carrier mobility, long diffusion lengths, and compatibility with low-cost fabrication techniques. Their investigation of $CH_3NH_3PbI_3Br$ absorber with NiOx as HTM and ZnO as ETM resulted in a fill factor of 75.96% and an efficiency of 16.12% [10].

Overall, these studies reveal a wide spectrum of approaches—ranging from absorber optimization and defect control to transport layer engineering and the exploration of lead-free materials—showing consistent progress in achieving high efficiency while moving toward more sustainable and environmentally friendly PSC technologies.

Chapter 03: Theoretical Study

3.1 Working Principle of Perovskite Solar Cell

The perovskite solar cell is one kind of photovoltaic (PV) technology that uses sunlight to create energy. They are based on a family of minerals called perovskites, which look similar to the mineral perovskite in terms of crystal structure. Perovskite solar cells represent a remarkable innovation in solar cell technology, with the potential to be more efficient than conventional silicon solar cells in terms of cost and efficiency. Even though they're still in the early stages of research, they've already reached outstanding efficiencies of over 25%, which puts them near the silicon cells' theoretical limit.

Essential factors for maximum effectiveness:

- Tunable Bandgap: By adjusting the material's composition, the bandgap of the perovskite material may be readily modified, enabling effective absorption of an extensive range of sunlight.
- Long Charge Carrier Diffusion Lengths: High efficiency demands that the electrons and holes in perovskite can travel an extensive distance before recombining.
- Low-cost Fabrication: Solution-processing techniques, which are significantly more straightforward and cheaper than the conventional processes used for silicon solar cells, can be applied to make perovskite solar cells.

Since all-solid perovskite solar cells (PSCs) were published in 2009, this technology has likely gained the most attention in photovoltaics. The number of published articles and the number of citations they received—more than 3,200 and 110,000, respectively, in only the most recent year (2017)- serve as evidence of this. Despite this intense research, the fundamental workings of these kinds of gadgets are still not fully understood. The publication by Ravishankar et al. will substantially contribute to this discussion since the authors have demonstrated that the final open circuit voltage, Voc, is largely independent of the work function of the electron-selecting layer.

3.2 Basic Structure of Perovskite Lead-Based and Lead-Free Perovskite Solar Cell

Conventional	Proposed
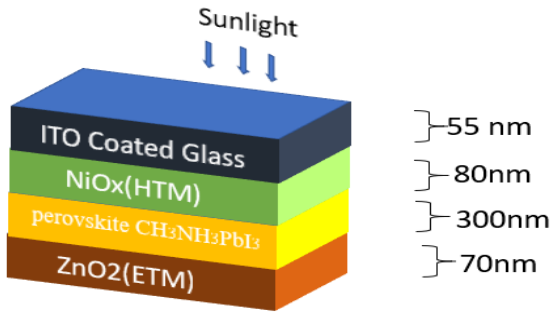	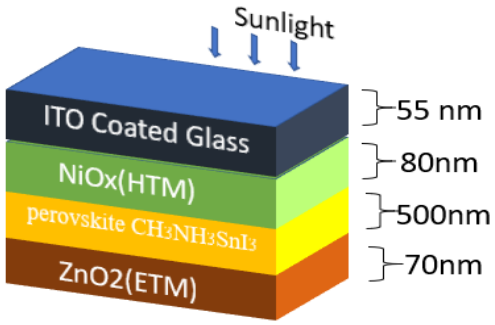
Structure of Perovskite CH3NH3SnI3	Structure of Perovskite CH3NH3SnI3

Fig 3.1 Basic structure of perovskite lead-based and lead-free perovskite solar cell.

Although the fundamental architecture of lead-based and lead-free perovskite solar cells remains the same, notable differences exist in the materials used for specific layers, as illustrated in Fig. 3.1.

1. Transparent Electrode: This layer allows incident light to enter the cell while collecting the generated current. It typically consists of fluorine-doped tin oxide (FTO) or indium tin oxide (ITO).

2. Hole Transport Material (HTM): HTMs extract and transport positive charge carriers (holes) from the perovskite layer to the transparent electrode. Common materials include Spiro-OMeTAD, PEDOT:PSS, and similar organic semiconductors.

3. Perovskite Absorber Layer: This central layer absorbs light and generates electron-hole pairs. Lead-based perovskites generally follow the ABX_3 structure ($A = MA^+$, $B = Pb^{2+}$, $X = I^-/Br^-/Cl^-$). Lead-free alternatives include tin-based or double perovskites.

4. Electron Transport Material (ETM): ETMs collect electrons from the perovskite layer and transfer them to the back electrode. Common examples include titanium dioxide (TiO_2) and PCBM.

3.2.1 Lead-based and lead-free perovskite solar cells differ in the following ways:

1. **Perovskite absorber material:** The absorber layer's makeup accounts for most variations. Lead (Pb) is present in lead-based perovskites, while lead-free substitutes employ other elements such as tin (Sn), bismuth (Bi), or double perovskite structures.
2. **Toxicity:** Lead is a hazardous substance, which raises questions about lead-based perovskite solar cells' potential risks to the environment and human health. Alternatives without lead solve this problem. However, there can be trade-offs in terms of stability and efficiency.
3. **Stability**: Lead-based perovskites may degrade over time, especially when exposed to heat and moisture. Research on lead-free substitutes is ongoing to increase their durability and long-term effectiveness.
4. **Efficiency:** Lead-based perovskite solar cells are now more efficient than most lead-free alternatives. On the other hand, lead-free material research is moving quickly forward, showing signs of an increase in efficiency that is on par with lead-based materials.

It's important to remember that every layer's exact components and concentrations might change based on the desired characteristics and solar cell arrangement. An overview of the fundamental components and significant differences between lead-based and lead-free perovskite solar cells is given in this review.

3.3 Characterizing Solar Cells and Building Solar Modules.

3.3.1: Current-Voltage Measurements

Current-voltage (J-V) measurements are fundamental for evaluating the performance of perovskite solar cells (PSCs). These measurements involve using a source measure unit (SMU) to record the current response of a solar cell under varying voltage biases, typically under standardized AM1.5 illumination. To ensure accuracy, an illumination mask is used to define the active area and prevent overestimation due to stray light. PSCs are known for their sensitivity to scan conditions and pre-measurement history, often exhibiting hysteresis between forward and reverse voltage sweeps. To mitigate this, stabilized current measurements or maximum power point tracking over a short duration are recommended. Reliable testing also requires transparent reporting of scan direction, rate, and preconditioning protocols. Leading journals mandate adherence to standardized testing

practices, including calibrated light sources, use of illumination masks, and declaration of spectral mismatches. Validation of short-circuit current density (JSC) via integrated quantum efficiency is also crucial for confirming accurate power conversion efficiency (PCE).

3.3.2 Photovoltaic Parameters

The performance of the solar cells is measured in terms of conversion efficiency, which is defined as the ratio of the output electrical power to the input optical power. However, this parameter depends on the sum of other essential parameters such as quantum efficiency (QE), short circuit current density (JSC), open-circuit voltage (VOC), Fill factor (FF), and maximum power (Pm)
Quantum efficiency (QE)= number of carriers collected/number of photons absorbed.

- Short circuit current density**, Jsc ≈ qG(Ln+Lp)** where Ln and Lp are the electron and hole diffusion lengths, given by L = √Dr, D is diffusion coefficient, and t is carrier lifetimes. (3.1)
- Open circuit voltage $Vo = \frac{nKT}{q} ln\left(\frac{I_L}{I_0} + 1\right)$ (3.2)
- Fill Factor, $FF = \frac{I_{mp}V_{mp}}{I_{SC}V_{OC}}$ (3.3)
- Maximum power, $nP_{max} = V_{OC}I_{SC}FF$ (3.4)
- Efficiency, $\eta = \frac{V_{OC}I_{SC}FF}{P_{in}}$ (3.5)

Where n is the diode ideality factor, k is the Boltzmann constant, T is temperature, q is the electronic charge, and It is the illuminated current. It is the reverse saturation current, and Imp and Vmp are the maximum current and voltage at the full power point. All the PV parameters are indicated in Figure 03, a typical current density-voltage curve of the solar cell.

All the PV parameters are illustrated in **Fig. 3.2**, which shows a typical current density–voltage (J–V) curve of a solar cell.

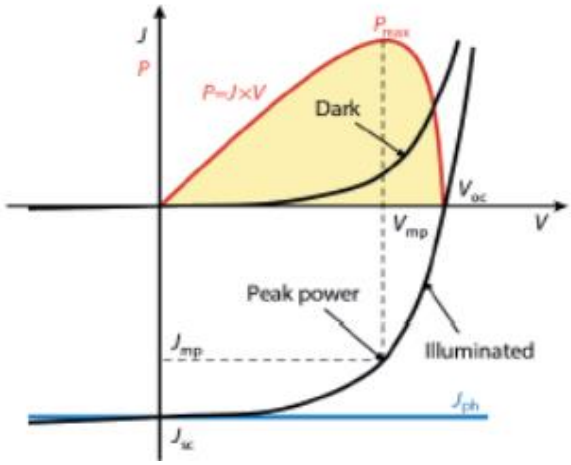

Fig 3.2 Typical illuminated current density-voltage (J-V) curve for a solar cell. J-V curve for the dark.

3.4 Solar Cell Recombination and Quantum Efficiency

External Radiative Efficiency (ERE) is defined as the proportion of total recombination events that result in photon emission. Although ERE is primarily important in light-emitting diodes, it also serves as an effective metric for solar cell performance, with higher ERE values indicating reduced nonradiative losses and potential for photon recycling. Perovskite solar cells can achieve ERE values up to 4%, surpassing those of conventional crystalline silicon (c-Si) cells.

Internal Quantum Efficiency (IQE) represents the ratio of extracted charge carriers to absorbed photons, accounting for losses in charge generation and transport within the absorber layer. In contrast, External Quantum Efficiency (EQE) quantifies the ratio of extracted carriers to incident photons across specific wavelengths

$$EQE(\lambda) = \frac{Jhc}{P(\lambda)e} \tag{3.6}$$

EQE includes losses due to reflection and parasitic absorption, typically from front-facing encapsulation and electrodes. Back-contact solar cell architectures reduce these losses by positioning charge-selective layers behind the absorber, enhancing optical and electrical performance.

3.5 Method of Selecting Suitable HTM & ETM

3.5.1 Energy Level Alignment:

- **NiOx**: Ensure the valence band maximum (VBM) of NiOx is higher than the HOMO level of your perovskite material (CH3NH3SnI3 in your case). This allows for efficient hole extraction towards the electrode.
- **ZnO_2:** Verify that the conduction band minimum (CBM) of ZnO_2 is lower than the CBM of your perovskite. This facilitates efficient electron extraction towards the electrode.

3.5.2 Mobility of Charge Carrier:

- **NiO_x:** To provide effective transport throughout the HTM layer and reduce recombination losses, search for NiOx variants with muscular hole mobility. One way to increase the mobility of the NiOx layer is to dope it.
- **ZnO_2:** Select ZnO2 with a high degree of electron mobility to enable effective charge transport in the ETM layer. It is possible to increase the conductivity of the ZnO_2 layer by annealing it.

3.5.3 Chemical and Thermal Stability:

- **NiO_x:** Both NiOx and ZnO2 are generally considered stable materials. However, ensure the NiO_x variant you choose can withstand processing temperatures and is resistant to moisture and UV light degradation.
- **ZnO_2:** Investigate the stability of your chosen ZnO_2 under operating conditions to ensure long-term device performance. Doping techniques might offer enhanced stability for some scenarios.

3.5.4 Interface Alignment:

- **NiO_x/Perovskite:** Optimize the contact between your perovskite and NiOx to reduce recombination losses. Buffer layers and surface treatments are examples of interface engineering approaches that can be useful.

- **ZnO_2/Perovskite:** For effective charge transfer, ensure adequate wetting and contact between ZnO_2 and the perovskite layer. Here, interface optimization techniques can also be used.

3.5.5 Additional Considerations:

- **Thickness:** Optimize the thickness of both NiO_x and ZnO_2 layers based on factors like charge transport, light absorption, and series resistance. Thicker layers might offer better transport but can increase resistance, while thinner layers might benefit light absorption but risk insufficient charge collection.
- **Processing methods:** Choose deposition techniques compatible with your chosen ETM and HTM materials, considering cost, scalability, and film quality.

3.6 Selecting of suitable absorber layer as a perovskite

Achieving high efficiency and stability in a perovskite solar cell (PSC) requires careful consideration when choosing an appropriate absorber layer. When making this decision, several considerations must be taken into account:

3.6.1 Properties and composition of the material:

- **Bandgap:** The bandgap of the perovskite material should be adjustable to match the sun spectrum for optimal light absorption. Formamidine lead iodide (FAPbI3), with a bandgap of 1.48 eV, and methylammonium lead iodide (MAPbI3), with a bandgap of 1.55 eV, are standard materials.
- **Charge carrier mobility:** Effective charge transfer within the absorber layer requires high electron and hole mobilities.
- **Charge carrier mobility:** Effective charge transfer within the absorber layer requires high electron and hole mobilities.
- **Stability**: For long-term device performance, the perovskite material must resist deterioration by heat, moisture, and UV light. Lead-based perovskites are fundamentally unstable, driving research into lead-free alternatives, including tin-based and bismuth-based perovskites.
- **Toxicity**: Lead in MAPbI3 presents health and environmental risks. Alternatives free of lead are the ones that should be commercialized.

3.6.2 Morphology And Crystallinity

- **Crystal structure:** The perovskite layer should have a consistent and well-defined crystal structure to reduce defects, and trap states obstructing charge transport and recombination.
- **Grain size:** Because larger grains have fewer boundaries between them and less scattering of charge carriers, they often function more efficiently. Grain size control can be difficult, though.

3.6.3 Processing Method :

- **Solution processing:** Spin-coating and blade coating are two easy-to-use, scalable, solution-based processes used to deposit most perovskite layers.
- **Compatibility with other layers:** The electron transport layer (ETL) and hole transport layer (HTL) in the PSC device stack should be able to work with the perovskite material and deposition technique.

Here are some additional factors to consider:

- Cost and availability of materials.
- Scalability of the fabrication process.
- Environmental impact of the materials and their production.

Choosing the suitable absorber layer for your PSC application requires careful consideration of these factors and ongoing research efforts to improve the performance and stability of perovskite materials.

By carefully selecting and optimising the absorber layer, researchers can push the efficiency limits of PSCs and make them a viable alternative to traditional silicon solar cells.

3.7 Effect of Bandgap, Thickness, Temperature, Electron Affinity, and Defect Density in Perovskite

3.7.1 Variations in Parameters' Impact on Perovskite Layers:

Because of their unique properties and massive potential in optoelectronic devices like solar cells, perovskite materials are attracting the attention of researchers. Several factors heavily influence their performance, and enhancing perovskite-based devices requires knowledge of these impacts. A summary of the effects you cited is as follows:

Bandgap:

- Directly impacts the range of light absorption. A more comprehensive range of light is absorbed by narrower bandgaps (lower energy difference between valence and conduction bands), which may increase efficiency. However, too little of a bandgap might result in voltage losses and thermal instability.
- Effects of carrier transport: Lower carrier mobilities from wider bandgaps often hinder charge collection and decrease efficiency.

Thickness:

- Thickness layer: absorbs more light. However, they may have increased recombination losses and decreased efficiency due to longer charge transport lengths.
- Thinner layers improve charge movement faster but may also negatively affect overall power generation and light absorption.

Temperature

- Higher temperatures typically cause quicker charge movement and increased electronic conductivity, which may increase efficiency.
- Excessive heat: can speed up non-radiative recombination, increase degradation, and ultimately decrease long-term device performance.

Electron Affinity (χ)

- establishes the energy level alignment between the nearby charge transport layers and the perovskite layer. Efficient charge extraction is made possible by optimal alignment, which reduces energy obstacles.
- Improper alignment: may impede extraction and lower efficiency by building energy barriers for charge carriers.

Defect Density

- As charge-trapping centres, defects reduce carrier lifetimes and increase non-radiative recombination, both of which hurt efficiency.
- Improving device performance and stability requires minimising fault density through carefully considered material development and manufacturing.

Additional Interplay

- These variables frequently interact and have an impact on one another. For instance, maintaining effective charge extraction may require modifying electron affinity to improve bandgap and thickness.

Summary

Development in optoelectronic devices depends on our ability to comprehend how different factors affect perovskite layers. Scientists are working to fully realise the potential of perovskite materials by customising their characteristics for particular uses via continuous research and development.

3.8 Selecting Suitable Bandgap And Thickness for Each Layer

ITO (Indium Tin Oxide):

- **Bandgap:** ITO is transparent in the visible and near-infrared range, so its bandgap doesn't play a significant role in solar cell performance. However, its thickness affects light transmission and sheet resistance. A typical thickness range for ITO in solar cells is 30-70 nm.
- **Thickness:** Consider a thickness of 50 nm for good light transmission and conductivity while minimizing parasitic resistance.

NiOx (Nickel Oxide):

- **Bandgap:** NiOx acts as the hole transporting layer (HTL) and should have a valence band maximum (VBM) higher than the perovskite HOMO level for efficient hole extraction. A suitable VBM for NiOx is around 5.4 eV. This translates to a bandgap of approximately 1.5-2 eV.

- **Thickness:** Thicker NiOx layers allow for better hole collection but can increase series resistance. A typical thickness for NiOx in perovskite solar cells is 10-20 nm. Consider 15 nm for a balance between good hole transport and minimal resistance.

$CH_3NH_3SnI_3$ (Perovskite):

- **Bandgap:** The optimal bandgap for the perovskite depends on the desired balance between light absorption and open-circuit voltage (Voc). CH3NH3SnI3 has a bandgap of around

1.1-1.2 eV, which allows for good light absorption across the visible spectrum but may lead to a lower Voc compared to perovskites with wider bandgaps. Consider this trade-off depending on your specific goals.

- **Thickness:** Thicker perovskite layers absorb more light but can increase carrier recombination losses. A typical thickness range for CH3NH3SnI3 in perovskite solar cells is 300-500 nm. Aim for a thickness around 400 nm for a balance between effective light absorption and efficient charge transport

ZnO (Zinc Oxide):

- **Bandgap:** ZnO acts as the electron transporting layer (ETL) and should have a conduction band minimum (CBM) lower than the perovskite CBM for efficient electron extraction. A suitable CBM for ZnO is around 4.0 eV, which translates to a bandgap of approximately 3.2-3.5 eV.

- **Thickness:** Thicker ZnO layers facilitate electron transport but can increase the risk of shunting (unwanted leakage current paths). A typical thickness for ZnO in perovskite solar cells is 20-40 nm. Aim for 30 nm for good electron transport while minimizing shunting potential.

3.9 Data table of different parameters

Table 3.1 Data table

Parameter	ITO Glass [6]	NiOx [6]	ZnO [6]	$CH_3NH_3SnI_3$ [4]	CH3NH3PbI [6]
Thickness (um)	0.055	0.080	0.070	0.500	0.5
Bandgap (eV)	3.5	3.5	3.2	1.3	1.55
Affinity (eV)	2.3	2.2	4.0	4.17	4.2
Dielectric permittivity (Er)	9	9	8.5	6.5	6.5
DOSCB (cm^{-3})	2.2×10^{18}	2×10^{18}	2.2×10^{18}	2.2×10^{19}	2.2×10^{19}
DOSVB (cm^{-3})	1.8×10^{19}	1.8×10^{19}	1.8×10^{19}	2.2×10^{19}	2.2×10^{19}
Electron mobility, un	3×10^{1}	4.7×10^{0}	1×10^{2}	1.6×10^{0}	2.0×10^{1}
Hole mobility, up	5	4.7×10^{0}	1×10^{3}	1.6×10^{0}	1.0×10^{1}
Donor concentration, ND (cm^{-3})	0	0	1×10^{16}	0	0
Acceptor Concentration, NA (cm^{-3})	2×10^{16}	5×10^{16}	0	3.2×10^{15}	1×10^{15}
Defect density, Nt (cm^{-3})	1×10^{15}	1×10^{15}	1×10^{15}	1×10^{13}	1×10^{13}

Summary

Table 3.1 presents the parameters of ITO, NiOx, ZnO, $CH_3NH_3SnI_3$, and $CH_3NH_3PbI_3$. ITO acts as a transparent electrode, NiOx as HTM, and ZnO as ETM. Absorber layers with lower bandgaps ensure light harvesting, while their lower defect densities compared to transport layers enhance performance by minimizing recombination losses.

Chapter 04: Research Methodology & Software Used

4.1 List of the Available Solar Cell Simulation Tools

4.1.1 Features of SCAPS -1D Software

SCAPS-1D is a one-dimensional simulation tool developed at the Department of Electronics and Information Systems (ELIS), University of Gent, Belgium, for modeling solar cell performance. Initially designed for CdTe and $CuInSe_2$-based devices, it now supports c-Si, GaAs, and a-Si technologies. Key features include:

• Support for up to seven semiconductor layers

• Graded optoelectronic parameters in compound semiconductors

• Interface and bulk defect definition

• Inter/intraband tunneling and recombination models (SRH, Auger, Radiative)

• J-V, C-V, C-F, and EQE analysis

• Batch execution, curve fitting, scripting, and result visualization

Its open-source availability and advanced features make it ideal for simulations in this thesis.

Action Panel

As shown in 4.1, the action panel is the first window that appears after executing the scaps.exe file installed on the PC. The central panel consists of different options (highlighted with the number that starts from 2 since the number 1 is already assigned to the main action panel). The user initially needs to click on the set problem to define the entire structure. After that, initial working points can be defined in terms of temperature, voltage, frequency and number of points. Here series and shunt resistance can be introduced to the simulated solar cell using the tool. The main pannel can also activate criteria for solar illumination or dark simulation. After defining the problem using the set problem and selecting the initial conditions, the user needs to visit the action setting to choose one or more desired analyses, including current-voltage (J-V), capacitance-voltage (C-V), capacitance frequency (C-f) and external quantum efficiency (EQE). The initial and final values for sweeping the parameter can also be set along with incremental steps regarding the number of points using the action setting panel.

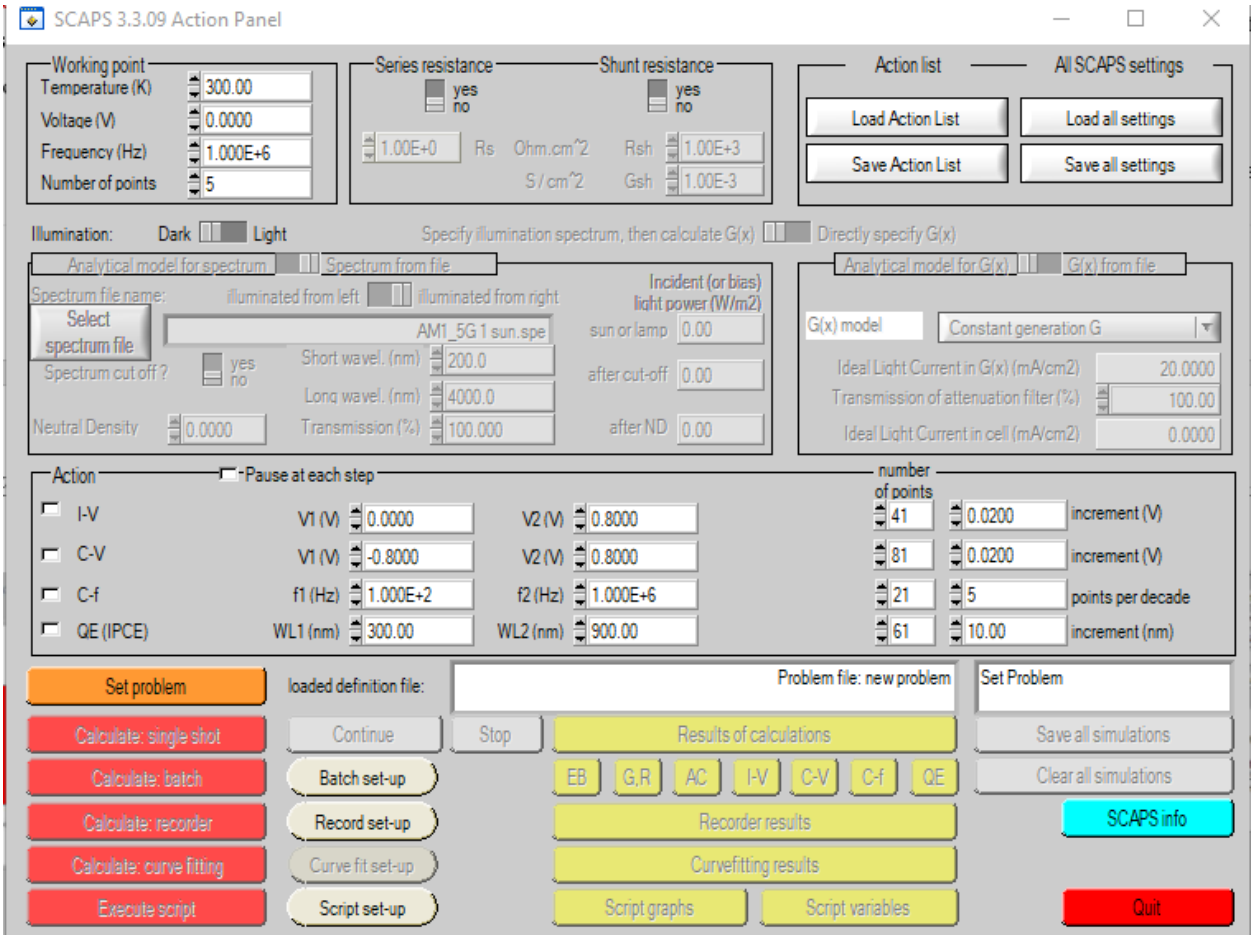

Fig 4.1 The main user interface of the SCAPS-1D solar cell simulator.

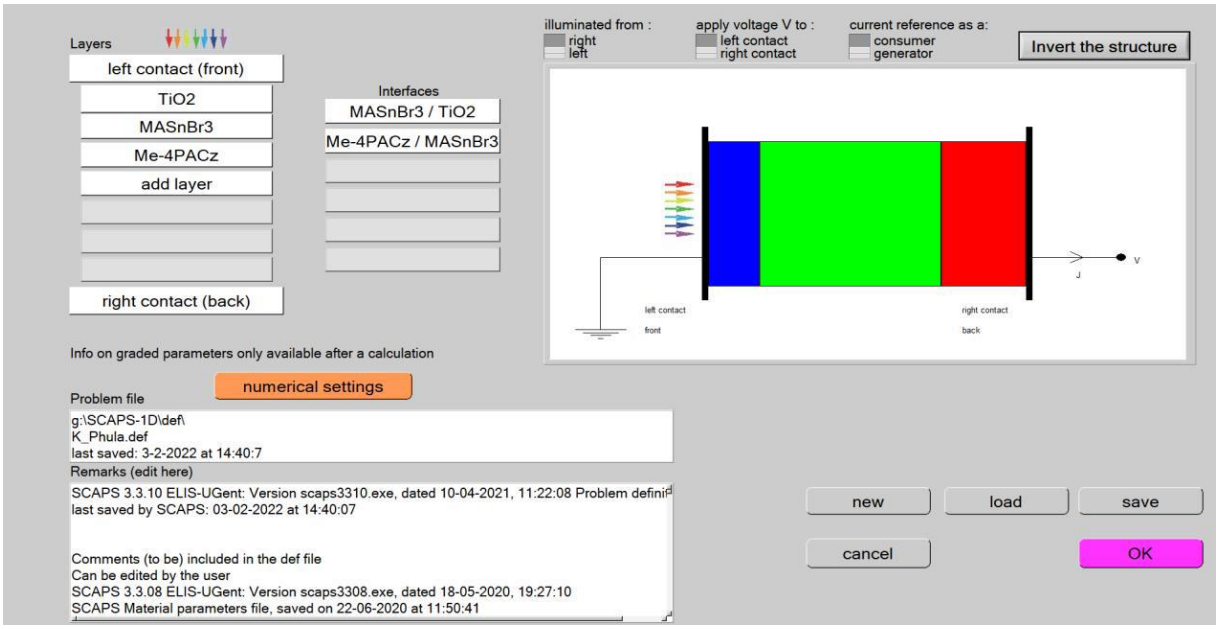

Fig 4.2 SCAPS-1D user interfaces for layer editing and solar cell definition.

Layer properties and save a material

It is essential to edit a layer's electrical and optical properties after adding the coating to ensure an accurate simulation for predicting the performance. The material properties can be obtained from literature and supplied using this panel shown in Fig. 4.3, which is activated after clicking the desired layer. Electrical properties can be adjusted in terms of band gap, affinity, dielectric contact, conduction and valence band density of state, thermal velocity, mobility, effective tunnelling mass, and doping. Coefficients for the recombination model and bulk defect density can also be supplied using this interface. The panel also allows us to select the absorption coefficient file from an external source or through inbuilt optical models. After inserting the desired properties, the user .3can save the material using the save material option. Already defined material held in the library of SCAPS-1D can also be invoked using the load material option. Once all the parameters are inserted, the user must click accept to return to the previous option.

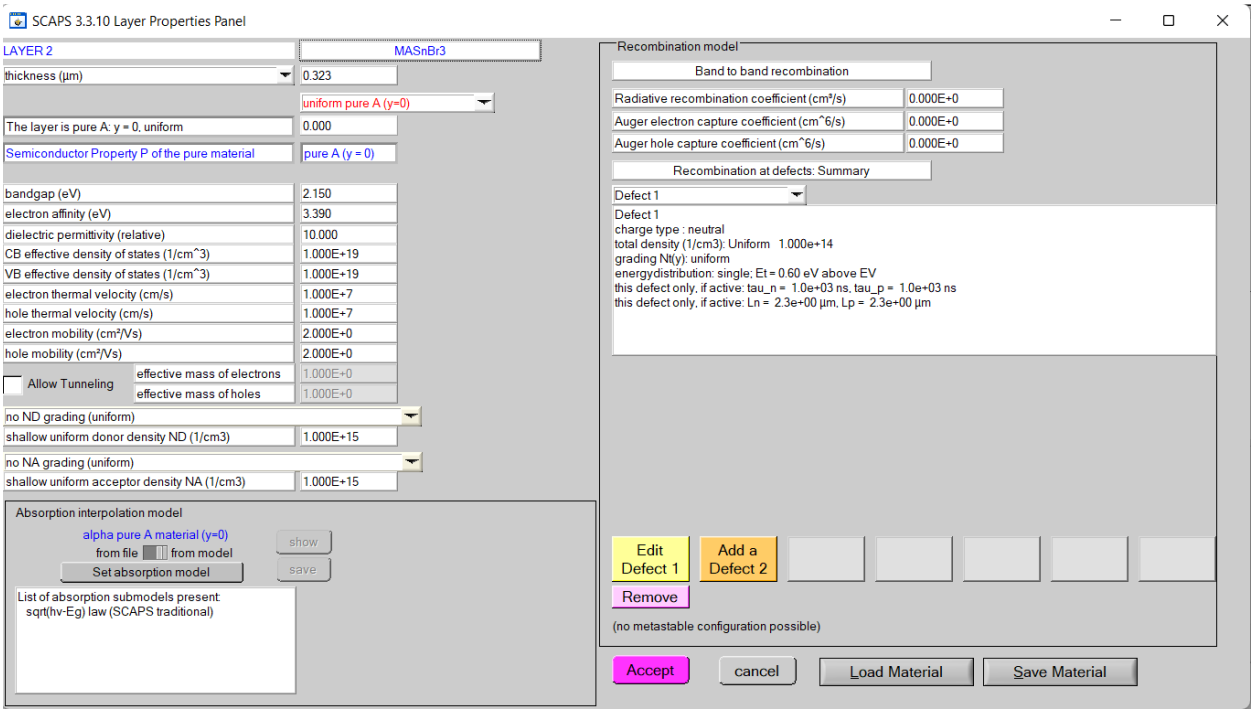

Fig 4.3 SCAPS-1D user interface for adding the optical and electrical properties for different layers.

4.1.2 Features of COMSOL Software.

A sophisticated software framework for modelling and simulating various physical events is COMSOL Multiphysics. Engineers, scientists, and researchers in multiple sectors use it, from medical devices and renewable energy to aerospace and automotive engineering.

Global parameters

Variables with a constant value throughout a simulation or parametric sweep are known as COMSOL global parameters. In basic terms, these are values that you can set and utilize wherever in your model as placeholders. They are, therefore, a successful instrument for increasing the flexibility and simplicity of your models.

COMSOL Global Parameters are a valuable tool for anybody using COMSOL Multiphysics to build flexible, reusable, and understandable models.

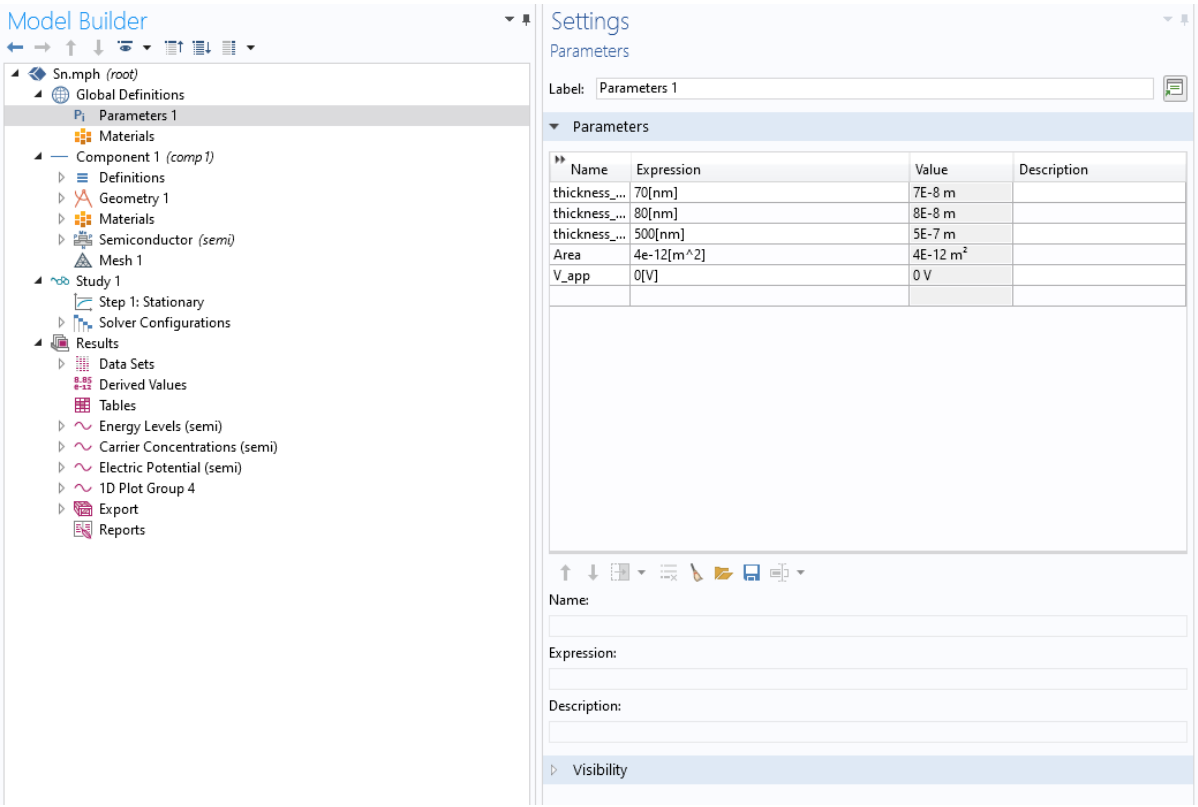

Fig 4.4 COMSOL user interface (Parameters Selection).

Geometry

- **Basis for your model:** The dimensions and form of the item or system you're modelling are specified by the geometry. It can take the form of primary forms like cylinders and spheres or complicated, multi-part designs with many interfaces.
- **COMSOL's flexibility**: The program supplies many methods for exporting and producing geometry.
    - Use built-in primitives like spheres, cylinders, and cubes.
    - Draw your geometry using CAD tools.
    - Import geometry from CAD files or other software.
- **Mesh matters:** COMSOL discretises your geometry into a mesh of individual components once you have it. Simulation accuracy is significantly improved because the governing equations are solved for every element in this mesh.

Materials:

- **Defining properties:** Materials specify the external features of the parts in your model. This covers mechanical, thermal, and electrical conductivity and density characteristics.
- **Preset or custom:** An extensive library of preset materials spanning a variety of applications is provided by COMSOL. Additionally, you can produce custom materials with features customized to your needs.
- **Material assignment:** You may assign a distinct material to each design section, enabling you to mimic intricate systems with numerous materials interacting.

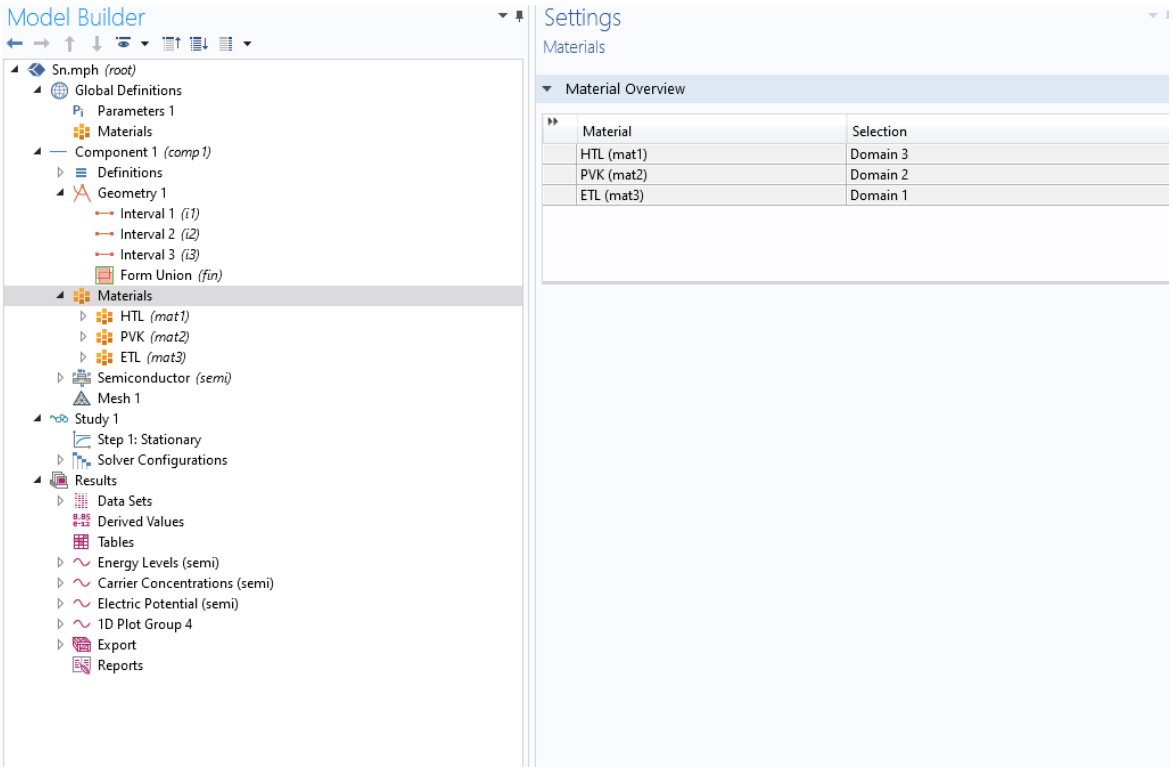

Fig 4.5 COMSOL user interface (Materials).

After solving a model, locate the Results branch in the Model Builder tree. This is your gateway to visualizing and analyzing simulation outcomes.

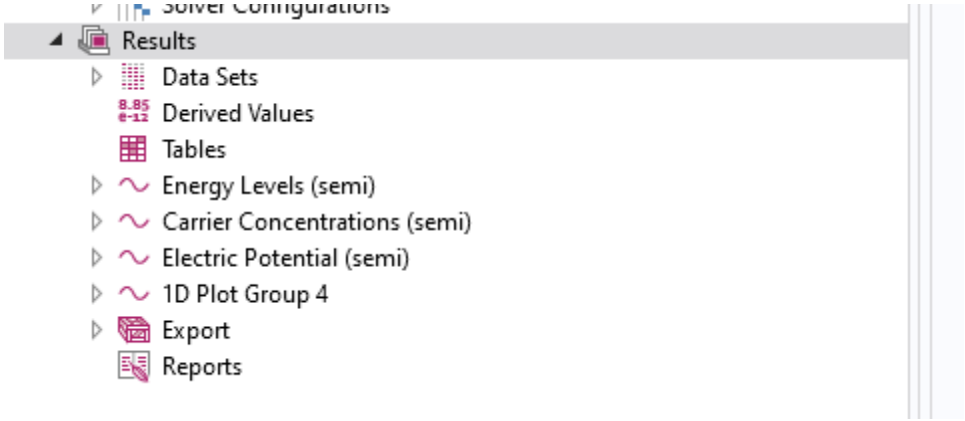

Fig 4.6 COMSOL user interface (Results).

4.1.3 Features of ORIGIN PRO Software

Here's a summary of what OriginPro is capable of:

- **Data management and import:** Bring in data in various forms, such as spreadsheets, text files, and scientific equipment. Use robust tools like data filtering, sorting, and transformations to organise and modify data easily.

- **Data Analysis:** Fit curves, analysis peaks, process signals, analysis images, and conduct various statistical studies. For complex analysis jobs, OriginPro provides add-on modules and built-in capabilities.
- **Charting and Illustration:** Use various 2D and 3D plot types to create suitable graphs and plots for publishing. Make your graphs unique by adding annotations, symbols, fonts, and colours.
- **Scripting and Automation:** Utilize Origin's scripting features to personalize your workflow and automate tedious activities. This allows you to create reports and analysis big datasets effectively.

4.2 Adopted Methodology

The methodology adopted in this thesis. Initially, literature is done to obtain the electrical and optical properties of the materials under consideration. After that, the design of the solar cell is done in SCAPS-1D using the features discussed above. Result sare obtained after designing the cell, and interpretation has been made. Standalone and tandem simulations are carried out in this thesis to fulfil all the objectives.

4.3 Modeling of Lead-Free Perovskite Solar Cell.

Perovskite solar cells have become more popular due to efforts to find cost-effective and environmentally friendly solar energy options. Of these, $CH_3NH_3SnI_3$ ($MASnI_3$) is a lead-free substitute that shows great promise and can reduce environmental risks associated with lead-based perovskites while still having a high efficiency. Modelling is essential to comprehend and maximize these new technologies.

A brief overview of the intriguing realm of $MASnI_3$ perovskite solar cell modelling is provided here:

4.3.1 Components and Structure of the Device:

A $MASnI_3$ perovskite solar cell typically consists of layers stacked over a transparent conductive substrate (such as indium tin oxide or ITO-coated glass). Among these levels are:

- **Layer of electron transport (ETL):** A thin layer called the electron transport layer (ETL) collects and transports electrons produced in the perovskite layer to the electrode. A popular ETL for $MASnI_3$ cells is SnO_2.
- **Perovskite active layer:** the centre of the cell, where electron-hole pairs are created by absorbing light. $MASnI_3$ absorbs a larger light spectrum, which might improve efficiency compared to lead-based perovskites.
- **Hole transport layer (HTL):** a thin layer that transfers holes created in the perovskite layer to the electrode by collecting and moving them. An extensively tilized HTL for $MASnI_3$ cells is spiro-OMeTAD.
- **Metal electrode**: Usually, the positive electrode is a thin coating of silver or gold.

4.3.2 Modeling Methodologies:

$MASnI_3$ perovskite solar cells may be simulated using a variety of software tools, each having benefits and drawbacks of its own. Popular options consist of:

- **SCAPS 1D**: a 1D simulation tool that aids in the optimization of essential settings like thickness and doping concentration and offers a fundamental knowledge of device physics.
- **COMSOL Multiphysics:** a robust finite element tool that enables the incorporation of variables like recombination, transport losses, and interface effects into more complex 3D simulations.

Despite existing challenges, significant progress has been made in modelling $MASnI_3$-based perovskite solar cells. These models have elucidated J-V characteristics, identified performance limitations, and guided novel material and device innovations. Continued advancements in modelling are essential for developing efficient, lead-free, and environmentally sustainable perovskite photovoltaic technologies.

Chapter 05: Simulation Result & Discussion

5.1 Performance Analysis

Both CH3NH3PbI3 (MAPbI3) and CH3NH3SnI3 (MASnI3) are promising materials for perovskite solar cells due to their tunable bandgaps, high light absorption coefficients, and long carrier diffusion lengths. However, they exhibit distinct advantages and disadvantages that impact their performance. Here's a comparative analysis:

MAPbI3: Has a bandgap of 1.55 eV, ideal for absorbing a broad range of sunlight in the visible region.

MASnI3: Possesses a wider bandgap (1.7 eV), potentially limiting light absorption in some portions of the spectrum.

MAPbI3: Can achieve certified PCEs exceeding 25%, making it the current champion material for perovskite solar cells.

MASnI3: Demonstrates lower PCEs, typically around 18-20%, primarily due to its limitations in light absorption and charge transport.

MAPbI3: General possesses higher carrier mobilities, facilitating efficient charge transport within the perovskite layer.

MASnI3: Can have lower carrier mobilities than MAPbI3, potentially leading to charge carrier recombination and reduced efficiency.

While MAPbI3 achieves higher PCE, stability and lead toxicity remain critical challenges. MASnI3, though less efficient, offers a stable, lead-free alternative, with ongoing research aiming to enhance performance and viability.

Table 5.1 Comparison between different perovskite parameters with the current study.

Perovskite Layer	ETM	HTM	Jsc	Voc	FF	PCE	Ref
CH3NH3PbI3	ZnO2	NiOx	20.94	1.06	81.79	18.22	[5]
CH3NH3SnI3	ZnO2	NiOx	32.55	0.97	81.06	25.73	This Work

5.2 Comparison Waveshapes J-V characteristics curve

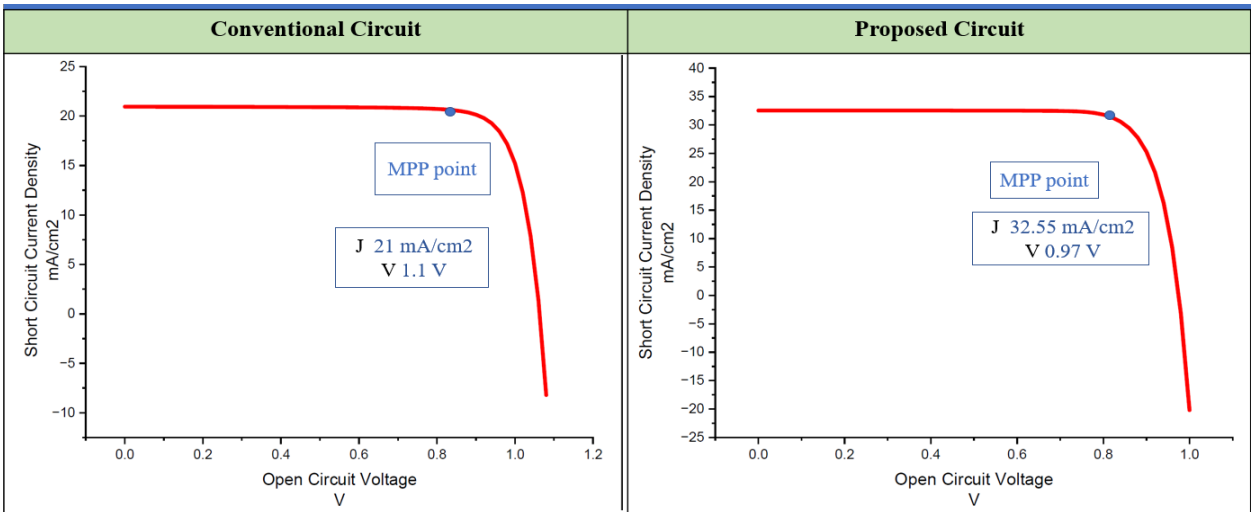

Fig 5.1 Comparison Waveshapes J-V characteristics curve

Open-Circuit Voltage (Voc):

- The Voc of the proposed circuit is greater than that of the conventional circuit. This suggests that during open-circuit conditions, the recommended circuit experiences less reverse leakage current, which results in a more considerable built-in potential and higher Voc.

Short-Circuit Current Density (Jsc):

- The suggested circuit has a greater Jsc than the traditional circuit. This implies that, compared to the typical circuit, the proposed circuit has either decreased light absorption or increased carrier recombination**.**

Maximum Power Point (MPP):

- In comparison to the typical circuit, the MPP of the suggested circuit seems to be at a lower voltage and current density. This means the proposed circuit may produce electricity at a lower maximum level.

Fill Factor (FF):

- The proposed FF is probably lower than the traditional circuit's. The J-V curve encloses a smaller rectangular region due to lower Jsc and MPP voltage.

5.3 Simulation result lead-based (Conventional).

This section shows the significant findings from the perovskite converter we selected for our thesis. These results are necessary to demonstrate that our results are equivalent to the authors' results.

5.3.1 Simulation Waveshape of the J-V Characteristics Curve.

We can find the desired value in the output section using simulation in the SCAPE 1D software. The bandgap and thickness values provided in the input section are the same as those found in the conventional. As said, the FF is 80.6, and the ETA is 18.22%. When compared to the value generated by the author, the VOC of 1.06 and Jsc of 23.34 in this conventional cell [21] are considered justified.

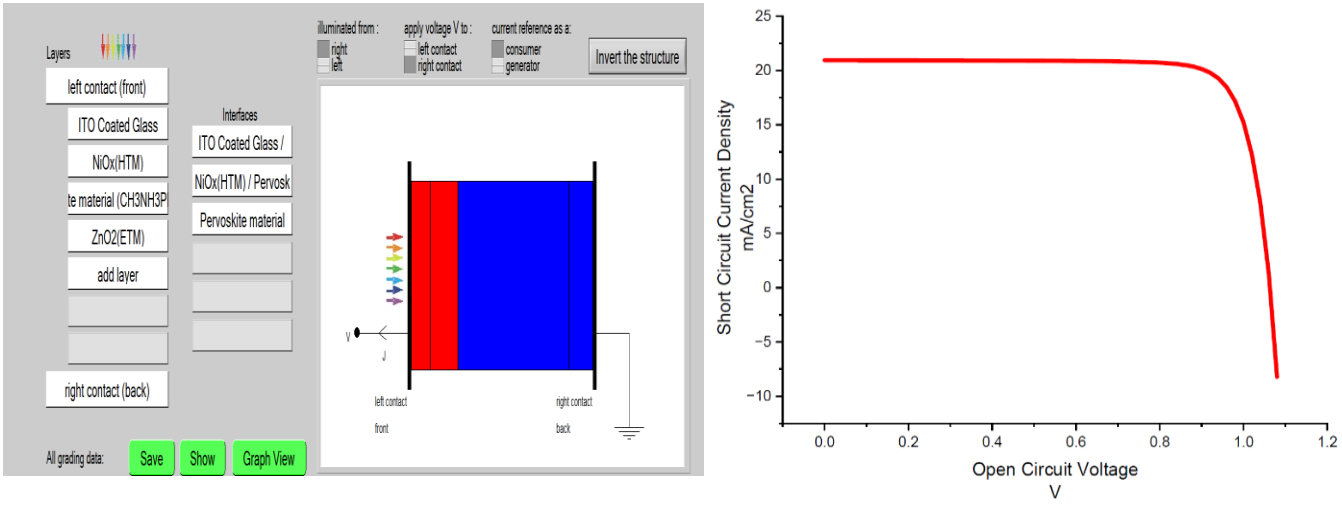

Fig 5.2 J-V characteristics curve of CH3NH3PbI3.

Table 5.2 Voc, Jsc, FF and ETA table of CH3NH3PbI3.

Voc (V)	Jsc (mA/cm2)	FF (%)	eta (%)
1.0633	20.944673	81.79	18.22

5.3.2 Simulation waveshape of the quantum efficiency curve.

In addition, the quantum efficiency of CH3NH3PbI3 is 95% when the wavelength is 360 nm, and the range of wavelength is 300 nm to 900 nm. When the wavelength is 800 nm, the QE is 0%, and at 300 nm, it is 75%.

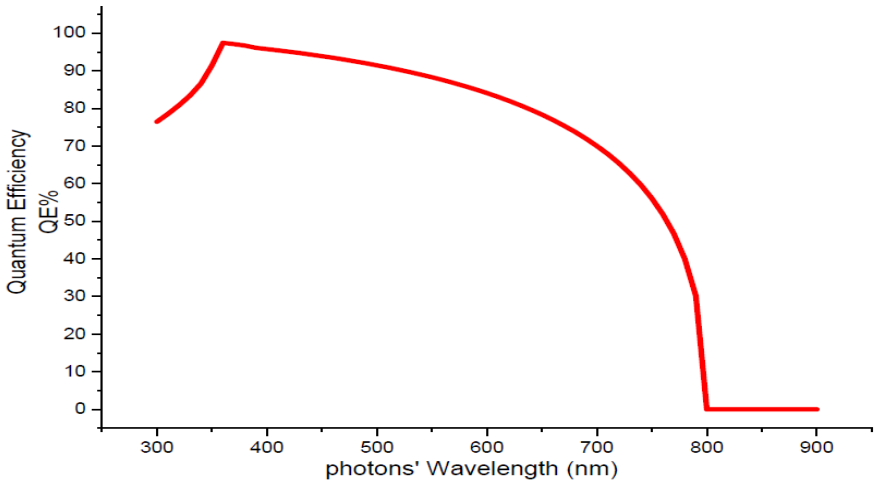

Fig 5.3 Waveshape of Quantum Efficiency CH3NH3PbI3**.**

5.3.3 Simulation waveshape of different Bandgap vs Efficiency

The band gap of the semiconductor material used to create a solar cell determines the cell's efficiency. To create a current, the band gap must be big enough to absorb enough sunlight but not so big that it prevents electrons from moving through the semiconductor and producing power. The solar cell can absorb more sunlight due to an enormous band gap. Efficiency and band gap do, however, come at a price. The electrons cannot flow through the semiconductor and generate energy if the band gap is too large. The ideal band gap for a solar cell is about 1.5 eV. The band gap of the semiconductor material used in the solar cell in the image is not given, but it is likely to be in the range of 1.2 to 1.7 eV.

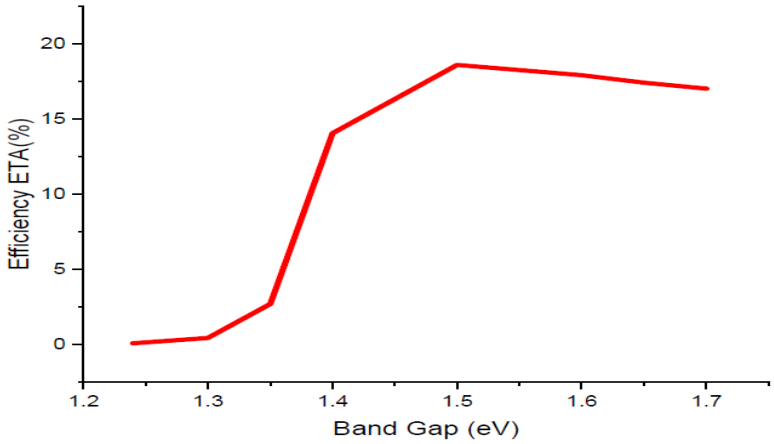

Fig 5.4 Waveshape of Bandgap vs Efficiency Curve.

5.3.4 Simulation waveshape of different Bandgap vs Fill Factor curve.

The curve reduces after a low initial value and a fast climb. The y-axis is labelled "Fill Factor FF (%)", ranging from 20 to 90%, while the x-axis is labelled "Band Gap (eV)," ranging from 1.2 to 1.7. Starting at roughly (1.2, 30%), the curve climbs sharply to about (1.4, 80%), levels off, and ends at around (1.7, 80%). A curve is defined as a smoothly-flowing continuous line that has bent. It does not have any sharp turns. The way to identify the curve is that the line twists and changes its direction at least once. , such as simple curves, non-simple curves, open curves, closed curves, upward curves, and downward curves.

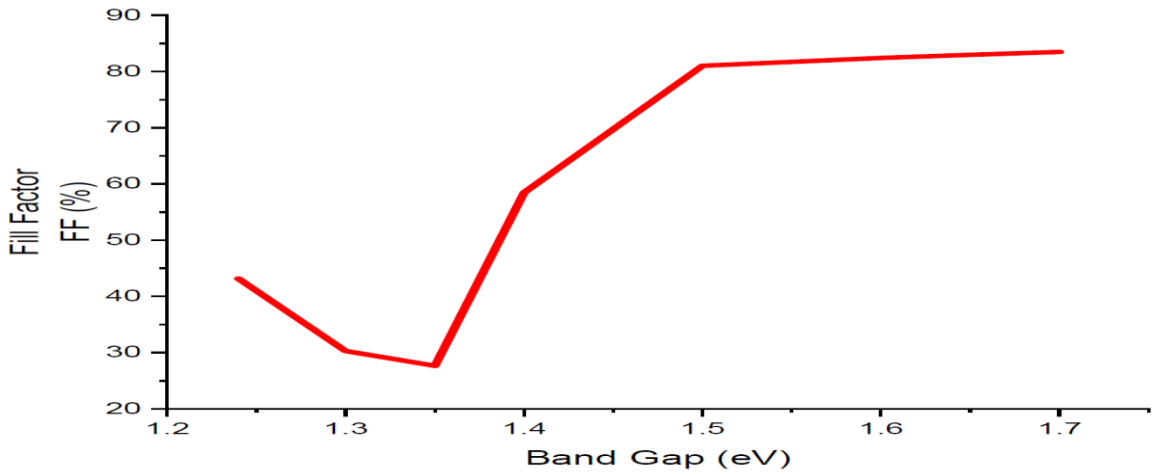

Fig 5.5 Waveshape of Bandgap vs Fill Factor Curve.

5.3.5 Simulation waveshape of different Thickness vs Efficiency curve.

As the thickness increases, the efficiency also increases. The x-axis is labelled “Thickness (MicroM)” and ranges from 0.20 to 0.45, and the y-axis is labelled “Efficiency ETA (%)” and ranges from 15 to 20%. A red curve on the graph represents a relationship between thickness and efficiency, showing an increase in efficiency as thickness increases. The curve is smooth and continuous, indicating a gradual change in values. A curve is defined as a smoothly-flowing straight line that has bent. It does not have any sharp turns. The way to identify the curve is that the line twists and changes its direction at least once.

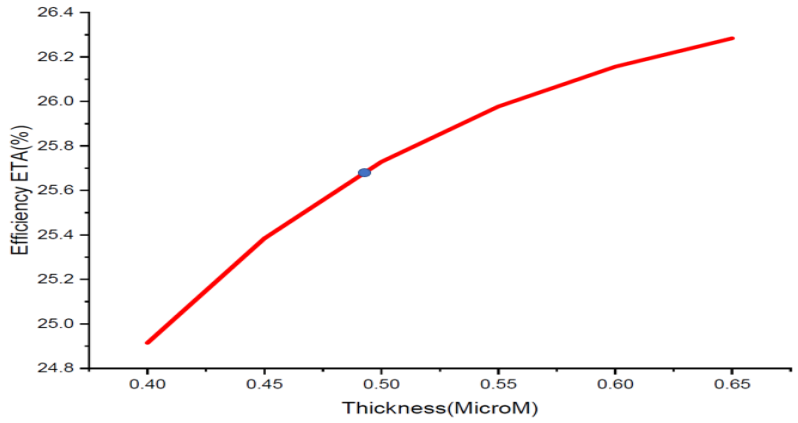

Fig 5.6 Waveshape of Thickness vs ETA Curve.

5.3.6 Simulation waveshape of different thickness vs fill factor curve.

The curve appears to show the effect of thickness on filtration. In this case, it looks like it's the filtration of ink through a membrane. The curve starts at around 82.15% fill factor for a thickness of 0.2 micrometres, decreasing as the thickness increases. By 0.4 micrometres, the fill factor is about 81.75%. This means that less ink can get through as the membrane gets thicker.

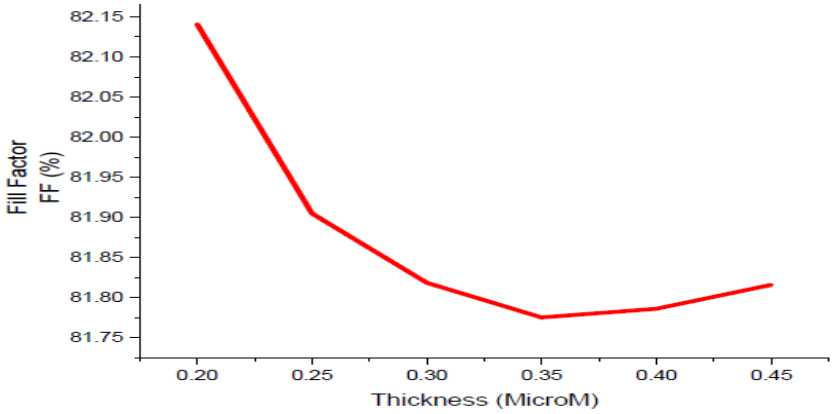

Fig 5.7 Waveshape of Thickness vs FF Curve.

5.3.7 Simulation waveshape of different electron affinity and efficiency curve.

The curve shows an increase in efficiency as electron affinity increases from 3.8 to about 4.1 eV, after which the efficiency decreases. The x-axis is labelled "Electron affinity (eV)", ranging from 3.8 to 4.3, and the y-axis is marked "Efficiency ETA (%)", ranging from 17.6% to 19.0%. The

curve starts at approximately (3.8, 17.6%), rises sharply to about (4.1, 19.0%), and then declines gradually. The curve shows a process's efficiency as a substance's electron affinity increases. Electron affinity is the energy released when an electron is attached to a neutral atom or molecule to form a negative ion. In this case, the process could create a chemical bond between the substance and another molecule, similar to conventional bonds.

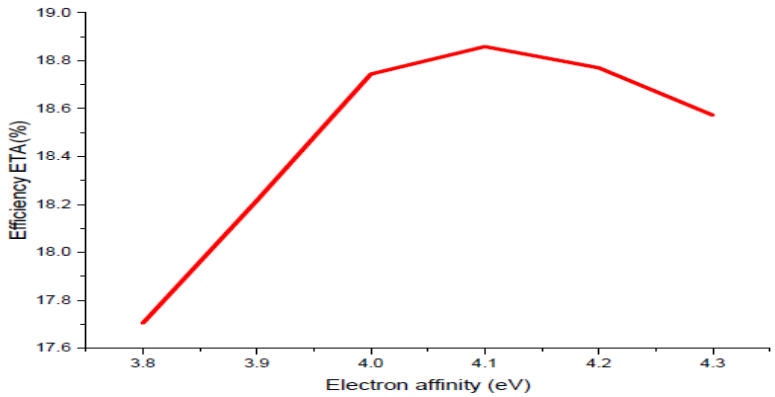

Fig 5.8 Waveshape of Electron affinity vs ETA Curve.

5.3.8 Simulation waveshape of different electron affinity and fill factor curves.

The curve starts at a low point, rises sharply to reach a peak, and then plateaus before beginning to decline slightly. The x-axis is labelled “Electron affinity (eV)”, ranging from 3.8 to 4.3, and the y-axis is tagged “Fill Factor FF (%)”, ranging from 78% to 84%. A red curve on the graph represents a relationship between electron affinity and fill factor, showing an increase in fill factor as electron affinity increases. The curve is smooth and continuous, indicating a gradual change in values.

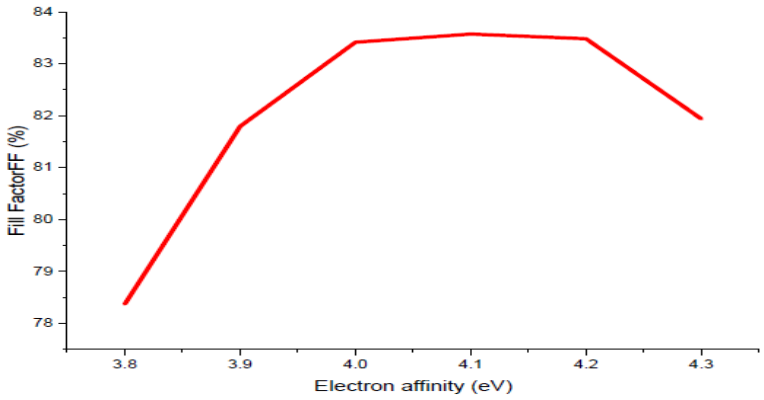

Fig 5.9 Waveshape of Electron affinity vs FF Curve.

5.3.9 Simulation waveshape of different temperature and efficiency curve.

As the temperature increases, the efficiency decreases. The x-axis is labelled “Temperature (K)”, ranging from 294 to 306, and the y-axis is labelled “Efficiency ETA (%)”, ranging from 18.0 to 18.5%. A red straight line represents the data, showing a decrease in Efficiency as Temperature increases. The curve is smooth and continuous, indicating a gradual change in values.

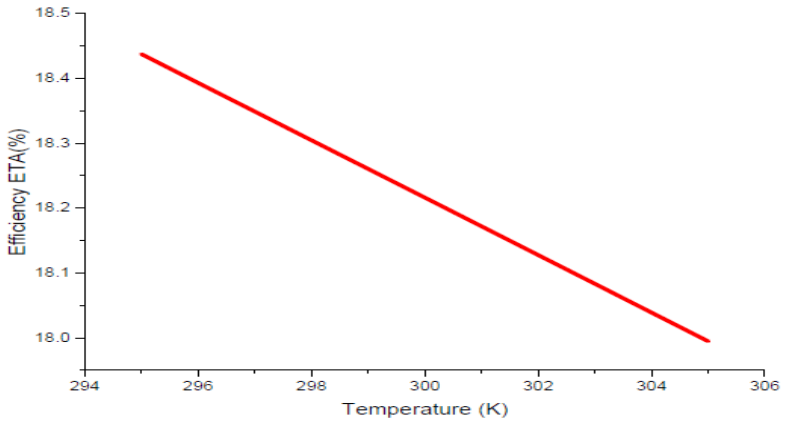

Fig 5.10 Waveshape of Temperature vs ETA Curve.

5.3.10 Simulation waveshape of different temperature and Fill Factor curve.

The curve is a straight line that slopes downwards, indicating a negative correlation between temperature and fill factor. As the temperature increases, the fill factor decreases. The x-axis is labelled “Temperature (K)”, ranging from 294 to 306, and the y-axis is labelled “Fill Factor (%)”, ranging from 81.5% to 82.1%. A straight red line represents the data, showing a decrease in the Fill Factor as Temperature increases.

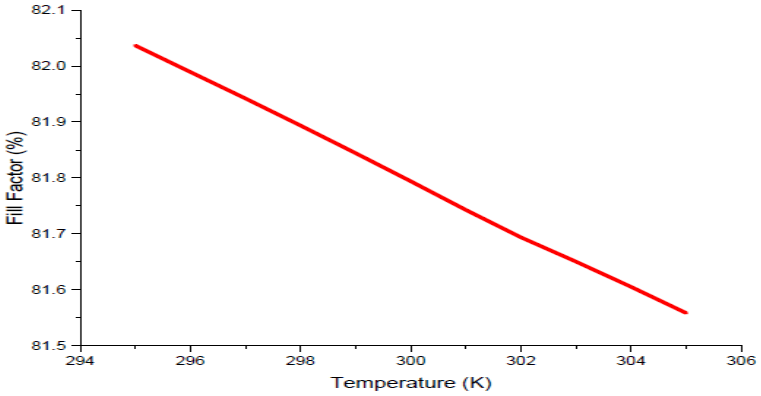

Fig 5.11 Waveshape of Temperature vs FF Curve.

5.4 Simulation result (Proposed)

This section presents all of the relevant results from the CH3NH3SnI3 (proposed) that are necessary to justify the purpose of the thesis.

5.4.1 Simulation waveshape of the j-v characteristics curve.

We can attain the appropriate efficiency and fill factor level at the output section by simulating the proposed layer in SCAPE 1D and COMSOL. This allows us to achieve our goal. We changed the absorber layer and used the CH3NH3SnI3 perovskite layer instead of CH3NH3PbI3. As previously mentioned, the Jsc is 23.2 mA/cm2. The circuit produced Jsc is 32.55 mA/cm2. Also, the Voc is 0.97V.

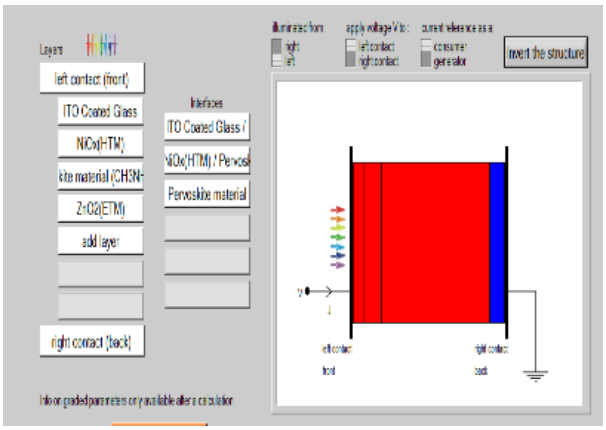

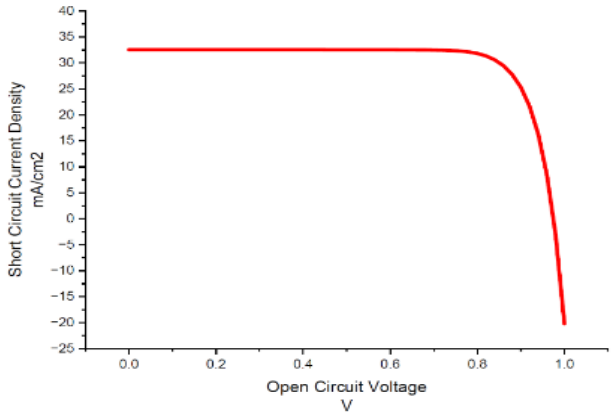

Fig 5.12 J-V characteristics curve of CH3NH3SnI3.

Table 5.3 Voc, Jsc, FF and ETA table of CH3NH3SnI3.

Voc (V)	Jsc (mA/cm2)	FF (%)	eta (%)
0.9750	32.551074	81.06	25.73

5.4.2 Simulation waveshape of the quantum efficiency curve.

The graph illustrates the variation in quantum efficiency (QE) with respect to photon wavelength. The QE begins near 0% at 400 nm, rises sharply to a peak of approximately 80% at 550 nm, and then gradually declines to around 20% at 800 nm. This trend reflects the decreasing photon energy

with increasing wavelength. Beyond a certain point, photons lack sufficient energy to excite electrons across the bandgap, resulting in reduced quantum efficiency.

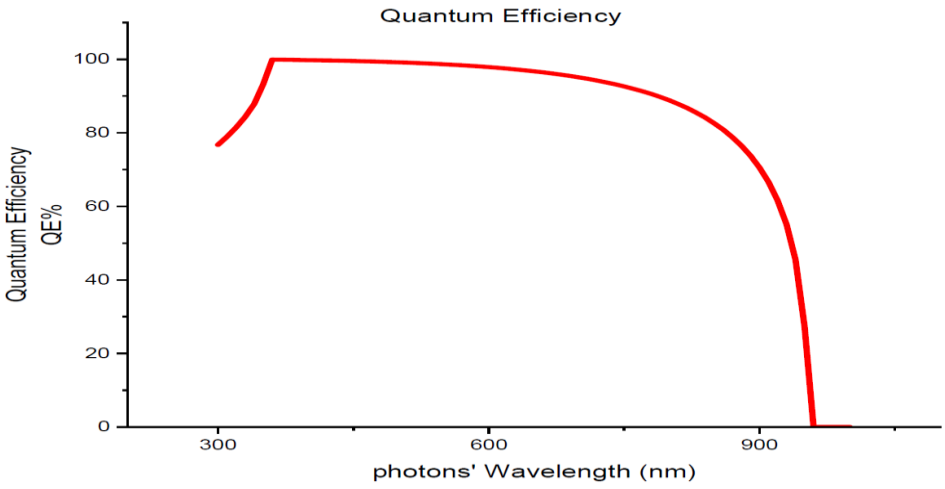

Fig 5.13 Waveshape of Quantum Efficiency CH3NH3SnI3**.**

5.4.3 Simulation waveshape of HTM of different Bandgap vs Efficiency curve

NiOx is employed as the hole transport material (HTM) for the $CH_3NH_3SnI_3$ absorber layer. The efficiency curve indicates a sharp decline as the band gap increases from 3.5 to 3.7 eV, aligning with the Shockley–Queisser limit, where the optimal efficiency is observed at a band gap of 3.5eV.

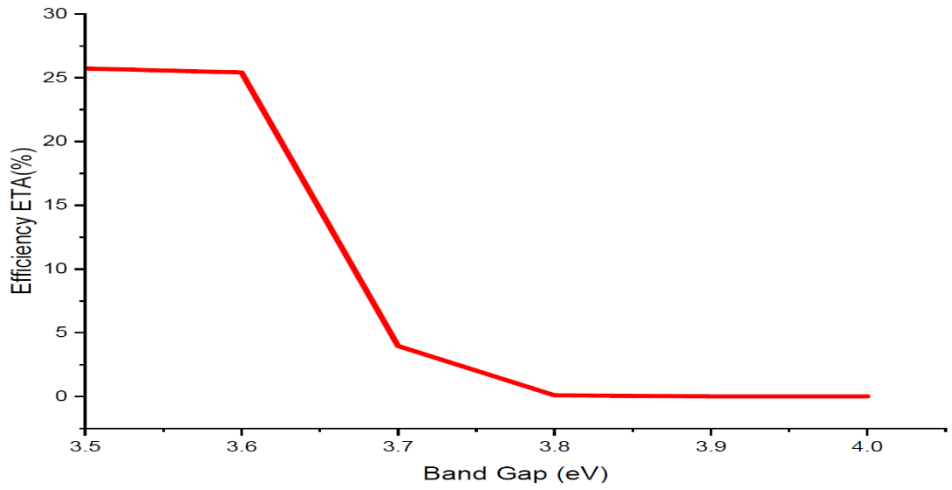

Fig 5.14 Waveshape of Bandgap vs ETA Curve of HTM.

5.4.4 Simulation waveshape of ETM of different Bandgap vs Efficiency curve

The graph illustrates the variation in solar cell efficiency with applied voltage for different bandgap ZnO Electron Transporting Materials (ETMs). Efficiency increases with bandgap up to a threshold, beyond which it declines. Notably, peak efficiency shifts with bandgap; for example, 3.5 eV ZnO ETM achieves ~18% at 1.0 V.

.

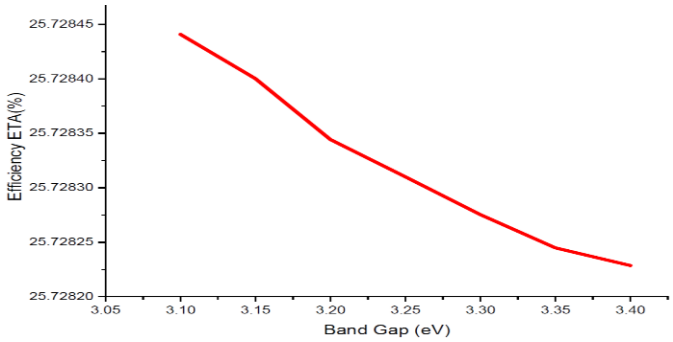

Fig 5.15 Waveshape of Bandgap vs ETA Curve of ETM.

5.4.5 Simulation waveshape of different Bandgap vs Efficiency curve, J-V curve, and table and curve.

The efficiency curves of $CH_3NH_3SnI_3$-based perovskite solar cells demonstrate a rise in efficiency with increasing absorber layer bandgap up to an optimal point, followed by a decline. Each curve reveals a distinct peak efficiency at a specific bandgap. For example, a 1.55 eV absorber peaks at 16.5% efficiency around 1.6 eV, while a 1.7 eV absorber peaks at 18% near 1.65 eV. This trend results from the balance between enhanced light absorption and reduced carrier mobility or collection at higher bandgaps.

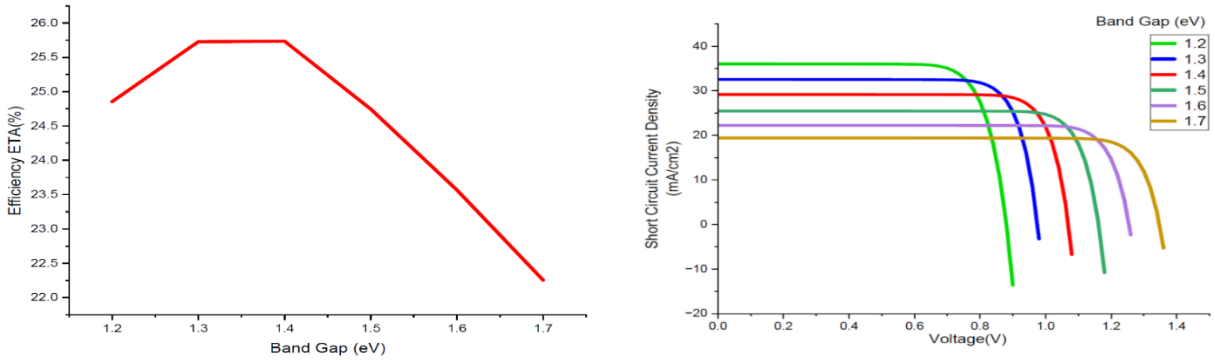

Fig 5.16 Waveshape of Bandgap vs Efficiency Curve and Optimization of Bandgap.

Table 5.4: I (mA/cm2) vs V characteristics with varying Bandgap

Band Gap (eV)	Voc(V)	Jsc(mA/cm2)	FF(%)	Eta(%)
1.2	0.88	36.03	78.35	24.85
1.3	0.97	32.55	81.06	25.74
1.4	1.06	28.27	82.96	25.73
1.5	1.16	25.45	83.67	24.75
1.6	1.25	22.24	84.45	22.98
1.7	1.34	19.41	85.03	21.21

5.4.6 Simulation waveshape of different bandgap vs fill Factor curve.

The figures illustrate that the fill factor (FF) of $CH_3NH_3SnI_3$-based solar cells initially increases with increasing absorber layer bandgap, reaches a maximum, and subsequently decreases. Each curve shows a unique peak FF at a specific bandgap—for example, the 1.55 eV absorber peaks at ~80% around 1.6 eV, while the 1.7 eV absorber peaks at ~82% near 1.65 eV. This behavior may result from improved light absorption and reduced recombination with increasing bandgap; however, excessively large bandgaps may hinder carrier mobility and collection efficiency, ultimately lowering the fill factor.

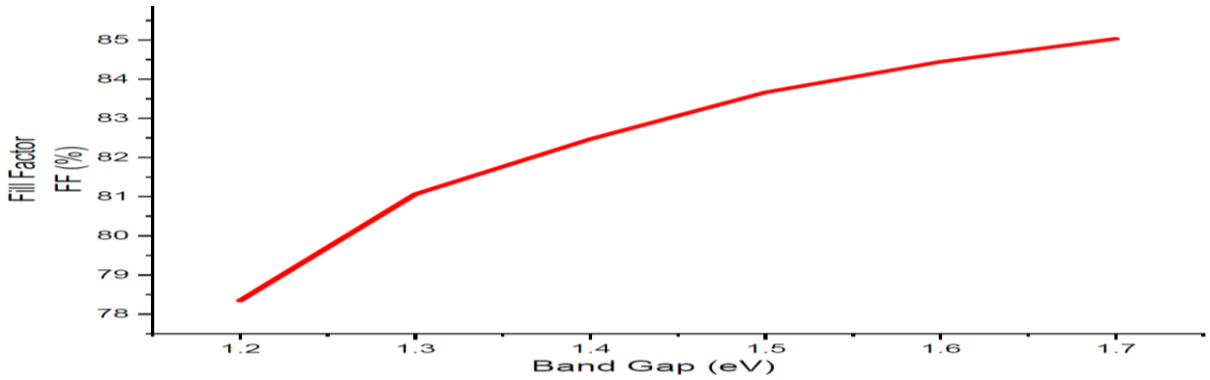

Fig 5.17 Waveshape of Bandgap vs FF Curve

5.4.7 Simulation waveshape of different thickness vs efficiency curve.

The curves demonstrate that the efficiency of $CH_3NH_3SnI_3$-based solar cells initially increases with absorber layer thickness, peaking at an optimal value, then declines. For example, 100 nm and 400 nm layers achieve peak efficiencies of ~12% and ~18% at 150 nm and 300 nm, respectively, due to competing absorption and recombination effects.

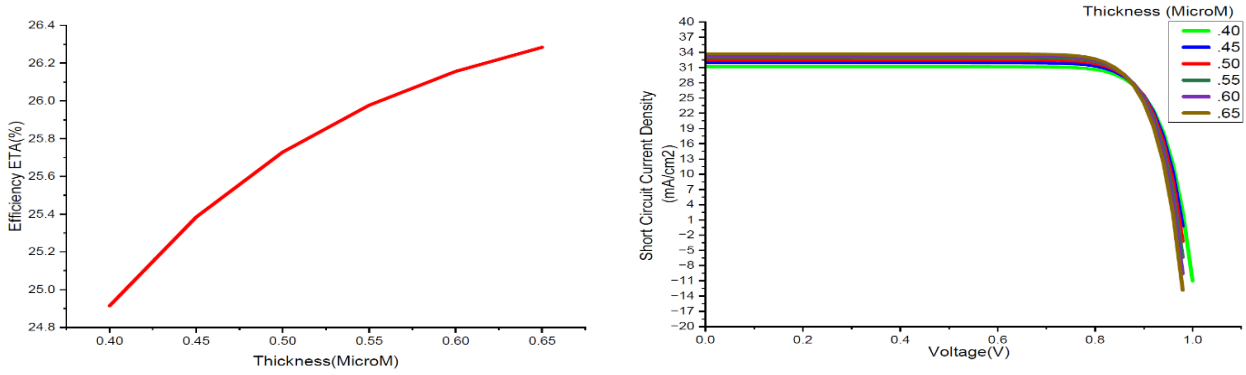

Fig 5.18 Waveshape of Thickness vs Efficiency Curve and Optimisation of Thickness.

Table-5.5: J (mA/cm2) vs V characteristics with varying Thickness

Thickness (microM)	**Voc(V)**	**Jsc(mA/cm2)**	**FF(%)**	**Eta(%)**
0.40	0.98	31.16	81.20	24.91
0.45	0.97	31.94	81.11	25.38
0.50	0.97	32.55	81.06	25.73
0.55	0.96	32.02	81.01	25.98
0.60	0.96	33.40	80.97	26.16
0.65	0.96	33.71	80.93	26.28

5.4.8 Simulation waveshape of different thickness vs fill factor curve.

Initially, as thickness grows, the fill factor rises to a maximal value. Following the apex, the fill factor falls as the thickness increases. For every curve, there is a tiny variation in the peak fill factor and the thickness at which it occurs; when the thickness is 75 nm, the 50 nm curve peaks at

around 74% FF. At 125 nm in thickness, the 100 nm curve peaks at about 78% FF. At 175 nm in thickness, the 150 nm curve peaks at around 79.5% FF. The 200 nm curve peaks at a thickness of 225 nm, or about 80% FF.

Enhanced light absorption: Greater light absorption by thicker absorber layers may result in higher current generation, raising the fill factor.

Decreased charge carrier transport: Electrons and holes must travel a greater distance to reach the electrodes as thickness increases. This may result in lower current generation and higher recombination losses, lowering the fill factor.

Additional factors: The link between thickness and fill factor may also be influenced by the qualities of the material, the interface, and the device's architecture.

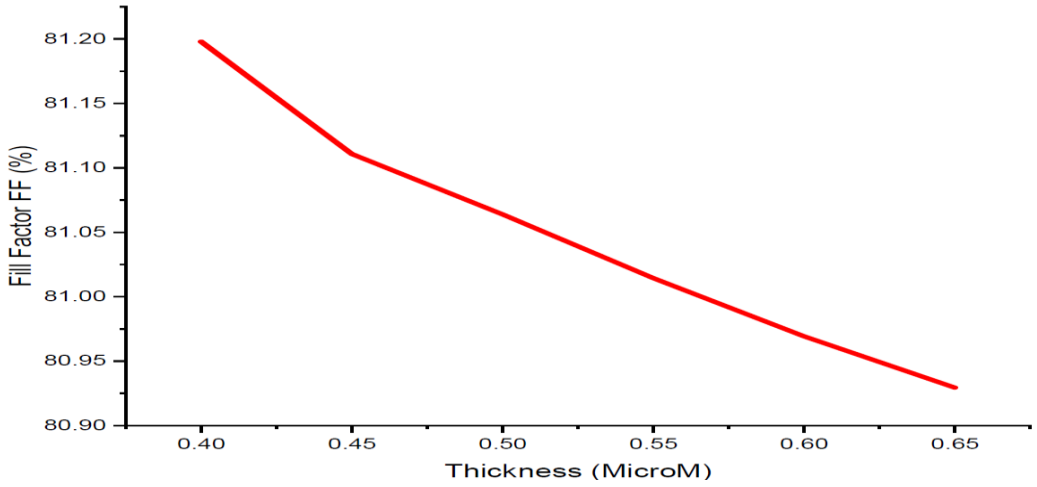

Fig 5.19 Waveshape of Thickness vs FF Curve.

5.4.9 Simulation waveshape of different electron affinity and efficiency curve.

The graph indicates that the efficiency remains low and constant as electron affinity increases from 3.7 eV to approximately 4.0 eV. However, beyond 4.0 eV, there is a sharp increase in efficiency up to about 30%. The graph is a two-dimensional plot with the x-axis labelled “Electron affinity (eV)” ranging from 3.7 to 4.2 and the y-axis labelled “Efficiency ETA (%)” ranging from 0% to 30%. The red line indicates the relationship between electron affinity and efficiency. The

efficiency remains constant at around zero from an electron affinity of 3.7 eV to just before reaching 4.0 eV. There's a steep increase in efficiency starting just before an electron affinity of 4.0 eV, reaching up to approximately 30% at around an electron affinity of slightly over 4.1 eV.

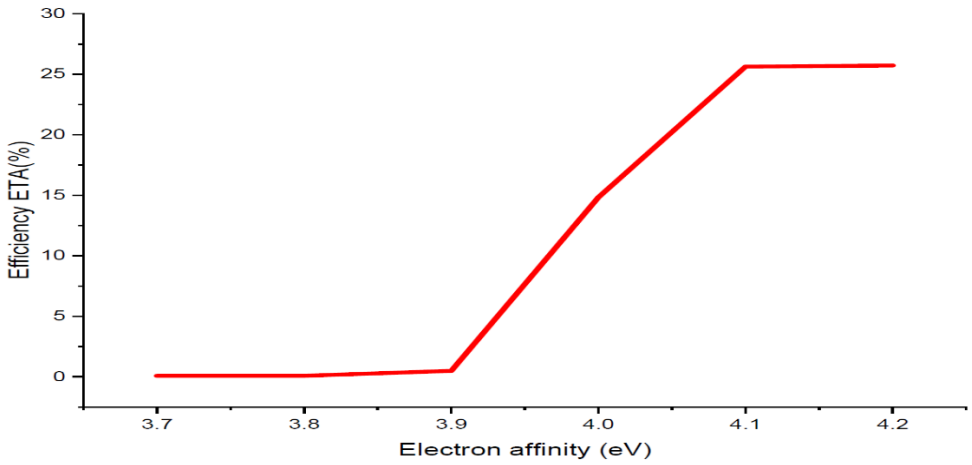

Fig 5.20 Waveshape of Electron affinity vs ETA Curve.

Chapter 06: Conclusion

6.1 Conclusion

This study presents a comprehensive analysis of enhancing the performance of lead-free perovskite solar cells by focusing on $CH_3NH_3SnI_3$ (methylammonium tin iodide) as the absorber layer. While conventional $CH_3NH_3PbI_3$-based devices have demonstrated commendable efficiency, the use of lead poses significant environmental and health risks. Tin-based alternatives offer a sustainable solution without compromising on performance. Through systematic simulation using SCAPS-1D, the $CH_3NH_3SnI_3$ structure—integrated with NiOx as the Hole Transport Material (HTM) and ZnO as the Electron Transport Material (ETM)—exhibited superior results after optimization. Specifically, the optimal bandgap of 1.3 eV and absorber thickness of 0.5 μm led to a power conversion efficiency (PCE) of 25.73%, with a fill factor (FF) of 81.06%, short-circuit current density (Jsc) of 32.55 mA/cm^2, and open-circuit voltage (Voc) of 0.97 V. These results highlight the immense potential of $CH_3NH_3SnI_3$ as a lead-free absorber, particularly when bandgap grading strategies are employed to maximize light absorption and charge carrier dynamics. Ultimately, the findings underscore the viability of tin-based perovskite solar cells as a safer and more efficient alternative to their lead-based counterparts. However, experimental validation through physical fabrication and real-world testing is essential to confirm the practical applicability of the proposed structure.

6.2 Future Work

Future research in perovskite solar cells focuses on developing alternative lead-free perovskite layers to achieve higher efficiency while maintaining environmental safety. Detailed analysis of absorber defect densities is essential to reduce recombination losses and enhance device performance. Additionally, improving the durability and stability of perovskite materials under environmental stresses such as heat and moisture is critical. These efforts aim to make next-generation solar cells more practical, reliable, and long-lasting.

6.3 References

[1] N. Singh, A. Agarwal, and M. Agarwal, "Numerical simulation of highly efficient lead-free all-perovskite tandem solar cell," *Solar Energy*, vol. 208, pp. 399–410, 2020.

[2] P. Roy *et al.*, "A review on perovskite solar cells: Evolution of architecture, fabrication techniques, commercialization issues and status," *Solar Energy*, vol. 198, pp. 665–688, 2020.

[3] S. Srivastava *et al.*, "Comparative performance analysis of lead-free perovskites solar cells by numerical simulation," *Journal of Applied Physics*, vol. 131, no. 17, 2022.

[4] M. A. Salih, M. A. Mustafa, and B. A. A. Yousef, "Developing lead-free perovskite-based solar cells with planar structure in confined mode arrangement using SCAPS-1D," *Sustainability*, vol. 15, no. 2, p. 1607, 2023.

[5] M. S. Rahman *et al.*, "Simulation based investigation of inverted planar perovskite solar cell with all metal oxide inorganic transport layers," in *2019 Int. Conf. Electr., Comput. and Commun. Eng. (ECCE)*, IEEE, 2019.

[6] A. Ghosh, S. Safat, and M. S. Islam, "Stable and efficient perovskite solar cell with metal oxide transport layers," in *2019 Int. Conf. Electr., Comput. and Commun. Eng. (ECCE)*, IEEE, 2019.

[7] P. P. Kumavat, P. Sonar, and D. S. Dalal, "An overview on basics of organic and dye sensitized solar cells, their mechanism and recent improvements," *Renewable and Sustainable Energy Reviews*, vol. 78, pp. 1262–1287, 2017.

[8] U. Mandadapu, S. V. Vedanayakam, and K. Thyagarajan, "Simulation and analysis of lead based perovskite solar cell using SCAPS-1D," *Indian J. Sci. Technol.*, vol. 10, no. 11, p. 65, 2017.

[9] J.-P. Correa-Baena *et al.*, "Promises and challenges of perovskite solar cells," *Science*, vol. 358, no. 6364, pp. 739–744, 2017.

[10] T. Wu *et al.*, "The main progress of perovskite solar cells in 2020–2021," *Nano-Micro Lett.*, vol. 13, pp. 1–18, 2021.

[11] Q. Jiang *et al.*, "Planar-structure perovskite solar cells with efficiency beyond 21%," *Advanced Materials*, vol. 29, no. 46, p. 1703852, 2017.

[12] M. A. Salih, M. A. Mustafa, and B. A. A. Yousef, "Developing lead-free perovskite-based solar cells with planar structure in confined mode arrangement using SCAPS-1D," *Sustainability*, vol. 15, no. 2, p. 1607, 2023.

[13] N. Singh, A. Agarwal, and M. Agarwal, "Numerical simulation of highly efficient lead-free perovskite layers for the application of all-perovskite multi-junction solar cell," *Superlattices and Microstructures*, vol. 149, p. 106750, 2021.

[14] S. P. Ray, P. Lohia, and D. K. Dwivedi, "Engineering in SnS-based solar cell for an efficient device with nickel oxide (NiO) as the hole transport layer," *Advanced Materials Letters*, vol. 12, no. 9, pp. 1–1, 2021.

[15] H. Abdulsalam and G. Babaji, "First Principle Study on Lead-Free CH3NH3GeI3 and CH3NH3GeBr3 Perovskite solar cell using FHI-aims Code," *Journal for Foundations and Applications of Physics*, vol. 6, no. 1, pp. 76–88, 2019.

[16] M. Q. Khan and K. Ahmad, "Origin and Fundamentals of Perovskite Solar Cells," in *Recent Advances in Nanophotonics-Fundamentals and Applications*, IntechOpen, 2020.

[17] O. A. Muhammed *et al.*, "Modeling and simulation of lead-free perovskite solar cell using SCAPS-1D," *East European Journal of Physics*, vol. 2, pp. 146–154, 2021.

[18] N. M. Ravindra and B. Prasad, "Saturation current in solar cells: an analysis," *Solar Cells*, vol. 2, no. 2, pp. 109–113, 1980.